5-2023

Uptake and Localization of Poly(2-vinyl-4,4-dimethyl azlactone) Modified with Rhodamine- and Coumarin-Based Molecules in Human Embryonic Kidney (HEK293) Cells

Garrett Tassin

Uptake and Localization of Poly(2-vinyl-4,4-dimethyl azlactone) Modified with Rhodamine- and Coumarin-Based Molecules in Human Embryonic Kidney (HEK293) Cells

by

Garrett Tassin

A Thesis
Submitted to the Honors College of
The University of Southern Mississippi
in Partial Fulfillment
of Honors Requirements

May 2023

Approved by:

Alex Flynt, Ph.D., Thesis Advisor,
School of Biological, Environmental and Earth Sciences

Jake Schaefer, Ph.D., Director,
School of Biological, Environmental and Earth Sciences

Sabine Heinhorst, Ph.D., Dean
Honors College

ABSTRACT

Fluorescence microscopy is a bioimaging technology that utilizes the excitation and emission of fluorophores to identify cellular structures, processes, and interactive events. Natural and synthetic organic dyes are frequently used in fluorescence microscopy techniques for imaging, therapeutic, and biomedical applications. It is also employed in the development of novel organic dyes for innovative methods of drug delivery and labelling. In this study, we investigate the behavior of an organic dye consisting of the post-polymerization modification of poly(2-vinyl-4,4-dimethyl azlactone) (PVDMA) with tetramethyl rhodamine cadaverine (TMR) and a coumarin-based molecule (DBAC). Using cultured HEK293 cells and fluorescence confocal microscopy, we show the dye preferentially localizes in lysosomal compartments within 10 minutes of incubation in cell culture. By comparing incubation times, we demonstrate how the dye experiences cleavage of its coumarin group and release into the cytosol with retention of the rhodamine group. Additionally, we co-stained the cells with LysoTracker Green DND-26 to quantify the degree of colocalization of the dye in lysosomes and cytosol. We show the rhodamine group has the highest colocalization with LysoTracker, and the colocalization of the coumarin group with LysoTracker and rhodamine is significantly reduced. This research elucidates the intracellular trafficking of the DBAC-TMR-PVDMA dye and provides necessary knowledge to further understand its behavior and develop an effective model for potential biomedical applications.

Keywords: Confocal microscopy, bioimaging, fluorescence microscopy, organic dye, localization, PVDMA

ACKNOWLEDGMENTS

First, I want to acknowledge and thank my thesis advisor, Dr. Alex Flynt, for allowing me the opportunity to join his lab. Working in his lab has been a tremendous learning experience, and I greatly appreciate the skills and knowledge I have gained from this opportunity.

Of course, I must express my immense gratitude to Iyanuoluwani Owolabi for being an integral part of this thesis project. I could not have completed this project without her incredible training and guidance since entering the cramped 5th floor culture room for the first time. Her trust in me instilled confidence in my potential as a writer and researcher, and her willingness to sit down and talk provided much needed respite on otherwise stressful days.

I also want to thank the Honors College at USM for granting me this experience and providing support throughout the process. Special thanks to Dr. Thomas Werfel at the University of Mississippi for providing me with the dye. In addition, I would like to thank Mississippi INBRE, the National Institutes of Health, and Mississippi EPSCoR: CEMOs for the facilities and funding that made my research possible.

Lastly, I'd like to thank my family and friends for being a constant source of support and encouragement since beginning this process my junior year.

TABLE OF CONTENTS

LIST OF ILLUSTRATIONS

LIST OF ABBREVIATIONS

ACQ	Aggregation-caused quenching
ATCC	American Type Culture Collection
BODIPY	4,4-Difluoro-4-bora-3a,4a-diaza-s-indacene
DBAC	2-Dimethylaminoethanol alkylated 3-bromoacetyl coumarin
DI	Deionized
DMEM	Dulbecco's Modified Eagle Medium
FBS	Fetal bovine serum
HEK293	Human embryonic kidney cells
PBS	Phosphate buffered saline
PVDMA	Poly(2-vinyl-4,4-dimethyl azlactone)
TMR	Tetramethyl rhodamine cadaverine

CHAPTER I: INTRODUCTION

Many bioimaging techniques enable non-invasive visualization of biological activity. Of the many technologies utilized for bioimaging, fluorescence microscopy is an effective and versatile tool. Fluorescence microscopy uses the excitation and light emittance of fluorophores to label and identify cellular or molecular targets (Kentner & Sourjik, 2010). Its advantages as an imaging technique are safety, sensitivity, non-invasiveness, and ability for modification in biological materials (Terai & Nagano, 2008). Fluorescence confocal microscopy is a bioimaging method that combines the advantages of fluorescence with the high resolution of precise lateral imagery (Ragazzi et al., 2014; Yang et al., 2016). Fluorescence confocal microscopy uses fluorophores to identify cell structures, localization, intracellular interactions, and other events in a thin two-dimensional image of the subject. It has seen applications in theranostics (Chandrasiri et al., 2020), chemo- and photothermal therapy (C.-E. Shi et al., 2019), organelle function analysis (Pendergrass et al., 2004), and clinical pathology (Ragazzi et al., 2014).

Among the fluorophores used in fluorescence microscopy, organic dyes are a popular agent owing to good biocompatibility, well-defined structures, ease of modification, and high sensitivity (Ding et al., 2018; Li et al., 2021; Qi et al., 2020; Shen et al., 2020). However, these dyes exhibit several qualities that limit their applications, such as poor solubility in water, short emission wavelengths, photodegradation, and a propensity for aggregation-caused quenching (ACQ) (Li et al., 2021; Qi et al., 2020). Due to the advantages and disadvantages presented by organic dyes, they see use in various methods for imaging or therapy functions. 4,4-Difluoro-4-bora-3a,4a-diaza-s-indacene (BODIPY) can create pure dye nanoparticles for phototherapy (Zhang et al., 2019),

cyanine and rhodamine can be loaded into nanoparticles for labelling (Miletto et al., 2010; Ren et al., 2020), and coumarin can form complexes with ionic species for chemical sensing (Khorasani et al., 2019).

Rhodamine is a group of related organic dyes frequently used as a fluorophore due to its excellent biocompatibility, bioavailability, and photostability under prolonged excitation (Grimm et al., 2020; X.-L. Shi et al., 2014; X.-F. Zhang et al., 2020). Rhodamine also exhibits desirable photophysical properties, such as high quantum yield, long emission wavelength, and high extinction coefficients (X.-L. Shi et al., 2014; X.-F. Zhang et al., 2020). A unique molecular characteristic of rhodamine is its spirocyclic ring form. Rhodamine is non-fluorescent in the closed spirocyclic form, but under acidic conditions, the ring opens, and rhodamine switches to a highly fluorescent form (Lv et al., 2013; Xia et al., 2021). This acidic-dependent ring opening reaction explains the propensity for rhodamine's use in the synthesis of pH and lysosome probes (Lv et al., 2013; X.-L. Shi et al., 2014; Xia et al., 2021; X.-F. Zhang et al., 2020).

Coumarin and its derivatives are a group of polyphenolic organic compounds originally isolated from the tonka bean, *Dipteryx odorata* (Akkol et al., 2020; Jain & Himanshu, 2012). Coumarin exhibits several clinically significant properties, such as anticoagulant, anticancer, antimicrobial, antifungal, and anti-inflammatory effects, and its derivatives are used as fluorescent dyes in labelling and phototherapy (Akkol et al., 2020; Jain & Himanshu, 2012). While unmodified coumarin is water insoluble and exhibits little fluorescence, numerous modified coumarin-based dyes have been produced with high quantum yields and great water solubility (Abdallah et al., 2019; Cao et al., 2019).

In this study, the uptake and localization of DBAC-TMR-PVDMA, a rhodamine and coumarin-based polymer dye, was examined by means of fluorescence confocal microscopy. The dye consists of a poly(2-vinyl-4,4-dimethyl azlactone) (PVDMA) backbone bound to tetramethyl rhodamine cadaverine (TMR) and 3-bromoacetyl coumarin alkylated with 2-dimethylaminoethanol (DBAC) (Figure 1).

In contrast to single-molecule dyes, the polymeric nature of PVDMA allows it greater production consistency, ease of modification, large scale synthesis, and controlled drug release (Sung & Kim, 2020). The objective of this research is to identify and understand the dye's behavior upon incorporation into human cells. Such information is necessary for potential researchers and manufacturers to create usable and safe therapeutic products based on the PVDMA model. As issues such as antibiotic resistance and increasing drug prices threaten the quality of therapies, it is imperative that we continue to create innovative, cost-effective, and efficient platforms for drug development. Polymeric drugs like PVDMA offer an exciting direction for new diagnostic and therapeutic tools, and understanding how they act in human systems is vital to our ability to provide medical care in a changing world.

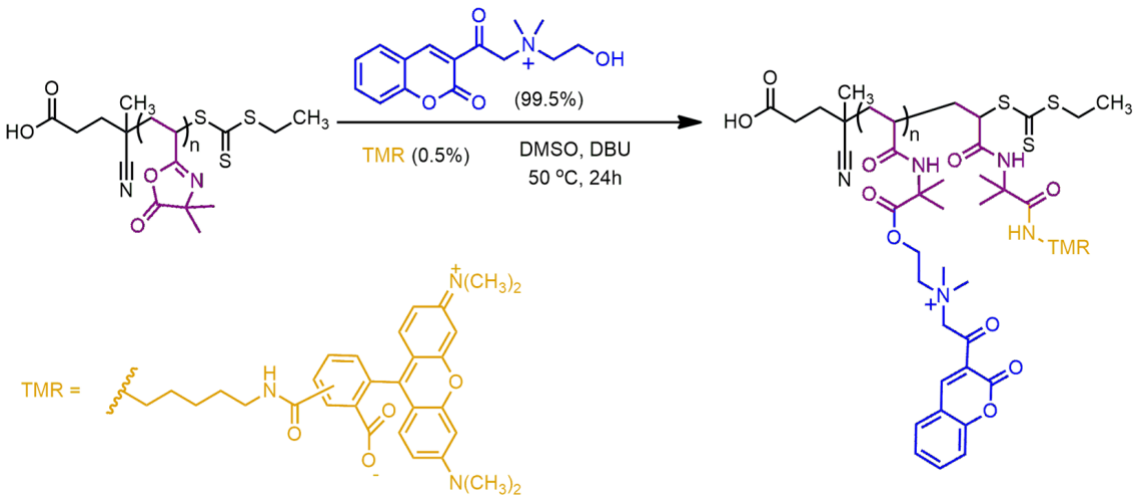

Figure 1. Schematic of DBAC-TMR-PVDMA synthesis. Synthetic pathway of DBAC-TMR-PVDMA by the post-polymerization modification of PVDMA with TMR and DBAC.

CHAPTER II: MATERIALS AND METHODS

Human embryonic kidney (HEK293) cells were used on this project due to the cell line's high reproducibility, reliability, and representation of cells in which the dye would be administered. HEK293 cells were acquired from ATCC (CRL-1573). HEK cells were grown under standard cell culture conditions (37° C, 5% CO_2, DMEM media with 10% FBS and 1% penicillin-streptomycin). In preparation for imaging, HEK cells were plated in glass bottom culture dishes. Cells were plated at a concentration necessary to reach approximately 70-80% confluence upon addition of the dye.

A stock solution of DBAC-TMR-PVDMA was prepared at a concentration of 1 mg/ml by dissolving 2 mg of dehydrated dye in 2 ml of deionized (DI) water. The dye was provided by Dr. Thomas Werfel's lab at the University of Mississippi. After the cells had reached approximately 70-80% confluence in the culture dishes, the dye was added to each dish at 50 µg/ml by adding 50 µl of the 1 mg/ml stock solution.

The dye was incubated for 10 minutes, 2 hours, and overnight on three separate occasions. Three dishes were incubated together for each incubation period. After incubation with the dye, cells were co-stained with 50 nM LysoTracker Green DND-26 (Invitrogen). Imaging of dye distribution in cells was done after the dye had completed incubating at its required time.

Immediately prior to imaging, cell media was removed from the culture dishes, and the cells were washed with 1 ml of PBS (Fisher Bioreagents). The PBS solution was prepared by dissolving two PBS tablets in 200 ml of DI water agitated with a magnetic spinner. Once the tablets were fully dissolved, 200 mL of DI water was added to the

solution to make the final concentration of 0.01 M PBS. Fluorescence and distribution of the dye was visualized with a Leica Stellaris STED confocal microscope.

Five replicate dishes were prepared and incubated with DBAC-TMR-PVDMA and LysoTracker Green DND-26 to determine the colocalization of both dyes. Colocalization values were collected for the rhodamine signal, coumarin signal, and LysoTracker as Pearson's correlations by the Leica Stellaris STED confocal microscope. The mean values of the five coumarin and rhodamine (CR), coumarin and LysoTracker (CL), and rhodamine and LysoTracker (RL) colocalizations and error bars were calculated and plotted using a Tukey ANOVA script. Statistical variance, standard deviation, and standard error were calculated by the script using the Rmisc, ggplot2, and multcomp functions.

CHAPTER III: RESULTS

Fluorescence confocal microscopy found that cellular uptake and localization of DBAC-TMR-PVDMA occurs most significantly in lysosomes (Figure 2). The coumarin and rhodamine-based molecules attached to the PVDMA backbone function as fluorescence signals at 405 nm and 573 nm, respectively. Fluorescence imaging of dye loaded cells showed colocalization between the coumarin and rhodamine signals. Varying dye incubation times did not have an apparent effect on the uptake of the dye (Figures 2a-c). However, the coumarin signal was observed accumulating in the cytosol of the cells after overnight incubation (Figure 2c). This behavior was not clearly seen with rhodamine signals even at up to overnight incubation.

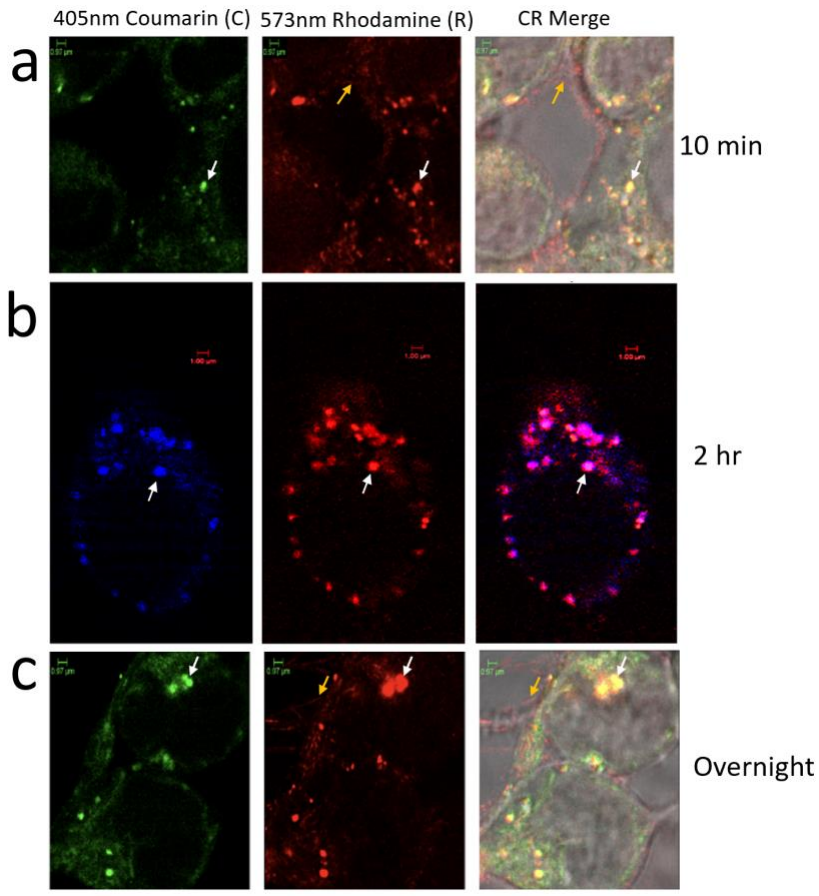

Figure 2. Confocal images of coumarin and rhodamine localization. Localization of coumarin (C) and rhodamine (R) signals after incubation periods of a) 10 minutes, b) 2 hours, and c) overnight. White arrows indicate colocalization of coumarin and rhodamine signals. Yellow arrows indicate filopodia-mediated uptake of dye. The green and blue colors of the 405 nm coumarin signal are visualizations of the same molecule.

Time-lapse images of treated cells show complete uptake and localized fluorescence of DBAC-TMR-PVDMA by 10 minutes of incubation (Figure 3). The fluorescent strength of the signals diminishes as they are visualized over the course of 60 minutes. Rhodamine signals are seen in the filopodia extensions of the cells without the presence of coumarin signals (Figure 3).

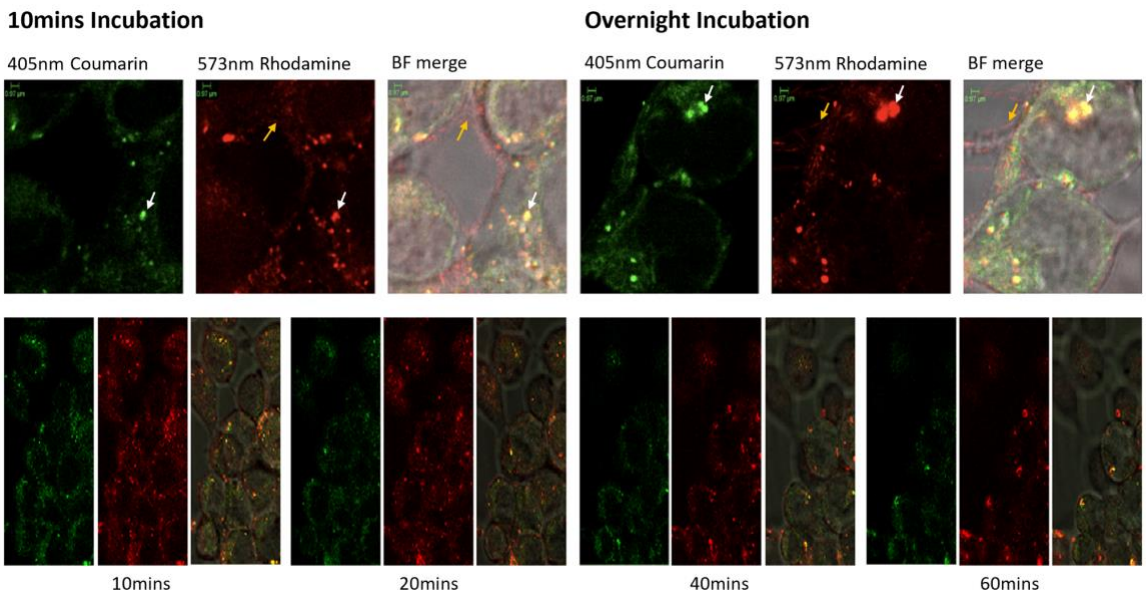

Figure 3. Coumarin and rhodamine localization and uptake. Time-lapse images were taken at 10 minutes, 20 minutes, 40 minutes, and 60 minutes after initiation of fluorescence imaging. White arrows indicate colocalization of coumarin and rhodamine. Yellow arrows indicate filopodia-mediated uptake of dye.

LysoTracker Green DND-26 (Invitrogen) is a BODIPY-based fluorescent dye that preferentially stains acidic cellular compartments, such as late endosomes and lysosomes (Mukherjee et al., 2022; Van der Velden et al., 2013). Imaging of cells loaded with DBAC-TMR-PVDMA and LysoTracker Green DND-26 showed varying levels of colocalization (Figure 4). The rhodamine signal and LysoTracker saw the greatest colocalization with a Pearson's correlation value of approximately 0.7 (Figure 5). The coumarin signal and LysoTracker produced a Pearson's correlation of about 0.62, and the rhodamine and coumarin signals experienced the least colocalization with a Pearson's correlation of less than 0.6 (Figure 5). Overlaps of the dyes support the calculated colocalization (Figure 4c).

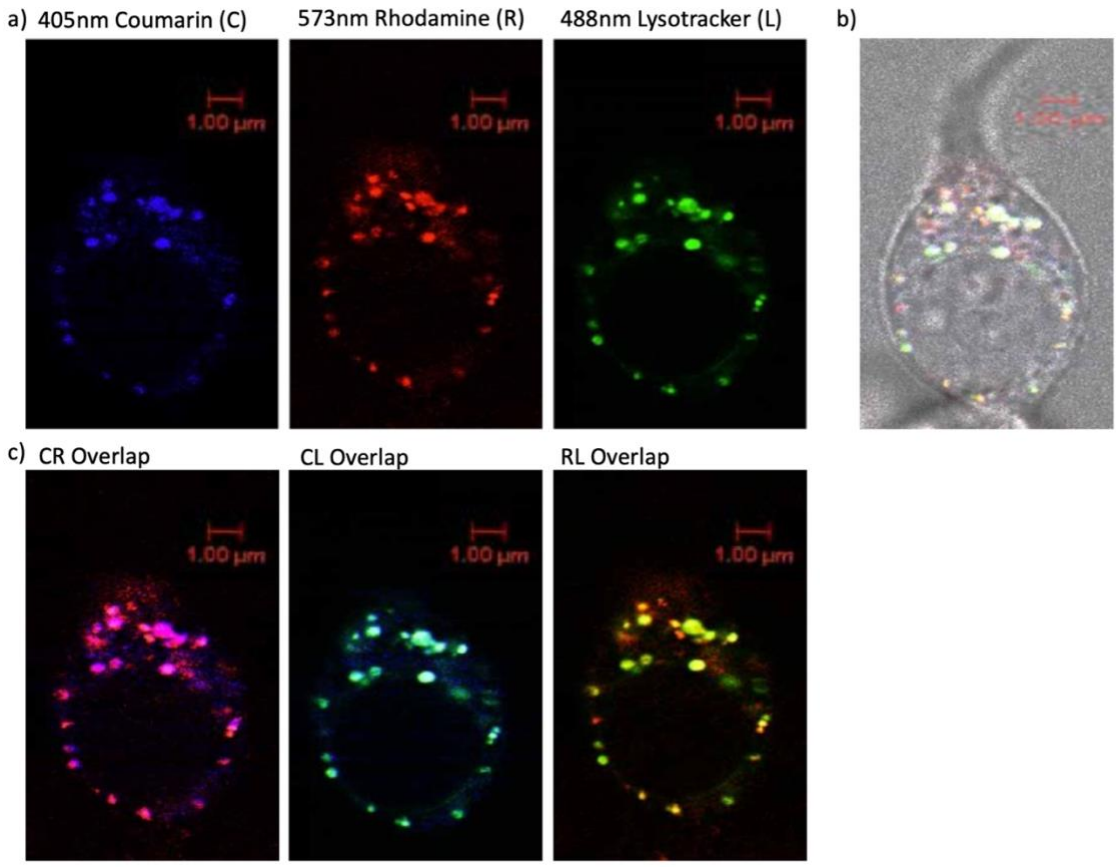

Figure 4. Localization of coumarin, rhodamine, and LysoTracker. a) Localization of coumarin (C), rhodamine (R), and LysoTracker Green DND-26 (L) in cells. b) Brightfield merge of C, R, and L. c) Overlaps of C, R, and L. Images were taken after 2 hour dye incubation in cells. LysoTracker was added 20 minutes prior to imaging.

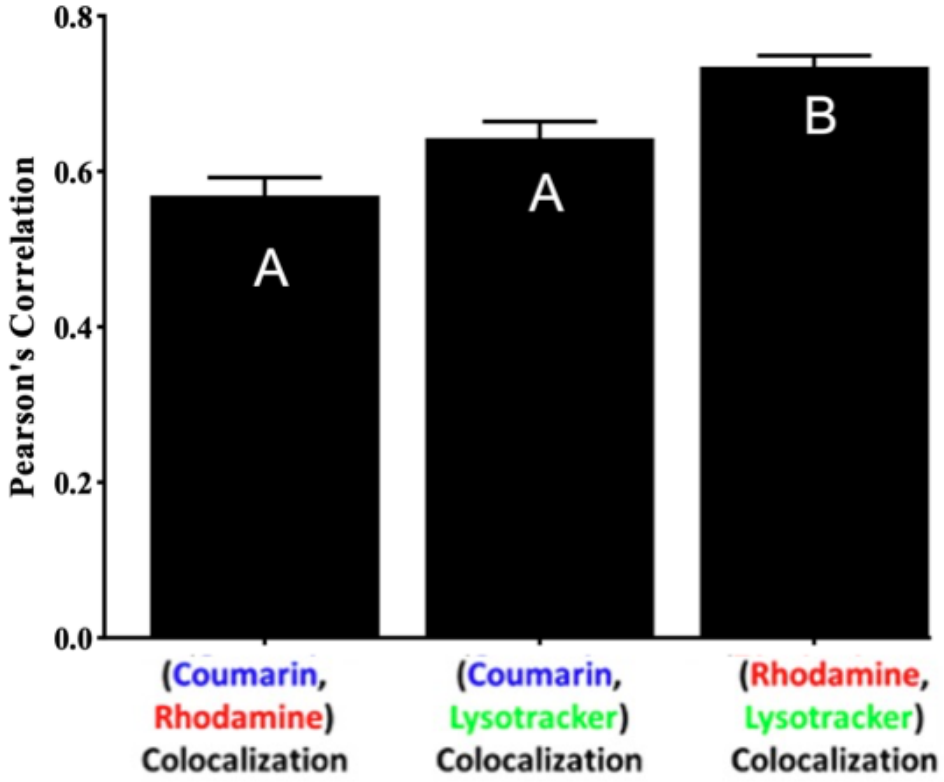

Figure 5. Colocalization of coumarin, rhodamine, and LysoTracker. Colocalization is based on average Pearson's correlation of the coumarin signal, rhodamine signal, and LysoTracker from multiple replicates. Pearson's coefficient values and error bars were calculated from the mean colocalization scores using a Tukey ANOVA script.

CHAPTER IV: DISCUSSION

Initial fluorescence imaging of DBAC-TMR-PVDMA showed some colocalization of the dye signals when incubated in cells. Comparing the images of cells incubated with the dye for 10 minutes, 2 hours, or overnight showed no discernible difference of the uptake and terminal localization of the dye. These findings, along with the time-lapse images taken over the course of an hour (Figure 3), demonstrate the ability of the dye to completely enter cells within 10 minutes of addition to culture and remain in the cells without escape for up to an overnight period. The fluorescence intensity of the rhodamine and coumarin signals is significantly reduced from the images taken at 10 minutes to 60 minutes (Figure 3). This behavior is due to an expected photobleaching of the fluorescent signals from prolonged light exposure. Since the dye can be visualized with full uptake and fluorescent strength at 10 minutes post addition to culture, the photobleaching effect is not significant to the performance of the dye.

The presence of rhodamine signal remnants in filopodia extensions (Figures 2 and 3) provides evidence of filopodia-mediated uptake as a mechanism of cellular entry. When HEK cells are grown as a monolayer, they connect with adjacent cells via filopodia extensions. Filopodia are used by some viruses for cell entry via endocytosis, and their dynamic actin remodeling produces ideal microenvironments for endocytic vesicle formation (Gallop, 2020; Heusermann et al., 2016). Interestingly, only rhodamine signals are found to remain in the filopodia with coumarin signals being fully localized in lysosomes or cytoplasm. The time-lapse images in Figure 3 show no cellular damage after exposure to the dye for over an hour. Similar conditions can be seen in the 2 hour and overnight incubation images (Figure 2). Though this is not a comprehensive

cytotoxicity test, the condition of the cells appears to demonstrate the safety and non-cytotoxicity of the dye.

Comparison of fluorescence images of rhodamine and coumarin with LysoTracker showed that both dyes localize in lysosomes, though at different rates and capacities. The approximately 0.7 Pearson's coefficient of rhodamine signals and LysoTracker shows that 70% of TMR in the cells is contained in lysosomes. Similarly, about 62% of coumarin signals are in lysosomes. Coumarin and rhodamine signals have a Pearson's coefficient of 0.57, sharing 57% colocalization in cells. With these values, it can be inferred that TMR largely localizes in lysosomes, and DBAC localizes in lysosomes to a lesser extent. DBAC appears to localize in the cytoplasm with more dispersion of fluorescence as compared to the relatively consistent spots of rhodamine signals. The greater fluorescence of rhodamine signals in images is supported by these findings since it is found in concentrated lysosomes instead of throughout the cytoplasm.

It is unknown why there is discrepancy between TMR and DBAC localization in the cells. TMR appears to have a greater affinity for the low pH environment of lysosomes. Previous studies have shown rhodamine to be an effective basis for creating pH and lysosome targeting probes (Lv et al., 2013; X.-L. Shi et al., 2014; Xia et al., 2021; X.-F. Zhang et al., 2020). Additionally, the fluorescence of rhodamine is dependent on its ring opening; a reaction that only occurs in low pH (Lv et al., 2013). Since DBAC was observed to accumulate in the cytoplasm largely without TMR, it can be inferred that DBAC must have separated from the PVMDA backbone and leaked into the cytosol. Coumarins have been shown to exhibit similar activity when synthesized to undergo photoinduced cleavage as dimers and in photocaging applications (Buckup et al., 2007;

Iturmendi et al., 2018; Schultz et al., 2022). These diverse behaviors of TMR and DBAC provide a possible explanation for the inconsistency of their localization in various areas of the cells.

The outcome of localization is also dependent on the uptake process of the dye. The exact nature of the uptake process is not known, but multiple possibilities can be explored. The two most likely routes are DBAC-TMR-PVDMA remains in early endosomes that become lysosomes before exiting to the cytoplasm, or it enters the cytoplasm and then is taken into lysosomes. If the condition of TMR's high affinity for low pH environments is accepted, both uptake processes can explain the data gathered in this study. In both scenarios, TMR is more likely to localize in the lysosomes with low pH while DBAC will preferentially exit to the cytoplasm. Further analysis of the molecular behavior of the dye is required to arrive at a definitive conclusion.

Based on fluorescence imaging of dye loaded cells and a comparison of colocalization of the dye signals, we have shown DBAC-TMR-PVDMA to be an effective polymer platform that can sustain modifications with small-molecule groups. The dye is completely loaded into cells by 10 minutes of addition to culture, and it largely remains sequestered in lysosomes after overnight incubation. However, the dye is not without error as DBAC is seen to leak into the cytosol, presumably from lysosomes where it is cleaved from the PVDMA backbone. This finding presents an interesting direction for further research into how DBAC's behavior can be used productively. Light-sensitive cleavage, targeted drug delivery, and coating as a protecting group are only some potential applications of DBAC. With high colocalization in lysosomes and a

potential method of delivery to cytosol, DBAC-TMR-PVDMA can be used as a format to inspire the development of interesting biomedical agents with varying abilities.

REFERENCES

Abdallah, M., Hijazi, A., Graff, B., Fouassier, J.-P., Rodeghiero, G., Gualandi, A., Dumur, F., Cozzi, P. G., & Lalevée, J. (2019). Coumarin derivatives as versatile photoinitiators for 3D printing, polymerization in water and photocomposite synthesis. *Polymer Chemistry*, *10*(7), 872–884. https://doi.org/10.1039/C8PY01708E

Akkol, E. K., Genç, Y., Karpuz, B., Sobarzo-Sánchez, E., & Capasso, R. (2020). Coumarins and coumarin-related compounds in pharmacotherapy of cancer. *Cancers*, *12*(7), 1959. https://doi.org/10.3390/cancers12071959

Buckup, T., Dorn, J., Hauer, J., Härtner, S., Hampp, N., & Motzkus, M. (2007). The photoinduced cleavage of coumarin dimers studied with femtosecond and nanosecond two-photon excitation. *Chemical Physics Letters*, *439*(4–6), 308–312. https://doi.org/10.1016/j.cplett.2007.03.076

Cao, D., Liu, Z., Verwilst, P., Koo, S., Jangjili, P., Kim, J. S., & Lin, W. (2019). Coumarin-based small-molecule fluorescent chemosensors. *Chemical Reviews*, *119*(18), 10403–10519. https://doi.org/10.1021/acs.chemrev.9b00145

Chandrasiri, I., Abebe, D. G., Loku Yaddehige, M., Williams, J. S. D., Zia, M. F., Dorris, A., Barker, A., Simms, B. L., Parker, A., Vinjamuri, B. P., Le, N., Gayton, J. N., Chougule, M. B., Hammer, N. I., Flynt, A., Delcamp, J. H., & Watkins, D. L. (2020). Self-assembling PCL–PAMAM linear dendritic block copolymers (LDBCs) for bioimaging and phototherapeutic applications. *ACS Applied Bio Materials*, *3*(9), 5664–5677. https://doi.org/10.1021/acsabm.0c00432

Ding, F., Zhan, Y., Lu, X., & Sun, Y. (2018). Recent advances in near-infrared II fluorophores for multifunctional biomedical imaging. *Chemical Science*, *9*(19), 4370–4380. https://doi.org/10.1039/C8SC01153B

Gallop, J. L. (2020). Filopodia and their links with membrane traffic and cell adhesion. *Seminars in Cell & Developmental Biology*, *102*, 81–89. https://doi.org/10.1016/j.semcdb.2019.11.017

Grimm, J. B., Tkachuk, A. N., Xie, L., Choi, H., Mohar, B., Falco, N., Schaefer, K., Patel, R., Zheng, Q., Liu, Z., Lippincott-Schwartz, J., Brown, T. A., & Lavis, L. D. (2020). A general method to optimize and functionalize red-shifted rhodamine dyes. *Nature Methods*, *17*(8), 815–821. https://doi.org/10.1038/s41592-020-0909-6

Heusermann, W., Hean, J., Trojer, D., Steib, E., von Bueren, S., Graff-Meyer, A., Genoud, C., Martin, K., Pizzato, N., Voshol, J., Morrissey, D. V., Andaloussi, S. E. L., Wood, M. J., & Meisner-Kober, N. C. (2016). Exosomes surf on filopodia to enter cells at endocytic hot spots, traffic within endosomes, and are targeted to the ER. *Journal of Cell Biology*, *213*(2), 173–184. https://doi.org/10.1083/jcb.201506084

Iturmendi, A., Theis, S., Maderegger, D., Monkowius, U., & Teasdale, I. (2018). Coumarin-caged polyphosphazenes with a visible-light driven on-demand degradation. *Macromolecular Rapid Communications*, *39*(18), 1800377. https://doi.org/10.1002/marc.201800377

Jain, P. K., & Himanshu, J. (2012). Coumarin: Chemical and pharmacological profile. *Journal of Applied Pharmaceutical Science*, *2*(6), 236–240. https://japsonline.com/admin/php/uploads/538_pdf.pdf

Kentner, D., & Sourjik, V. (2010). Use of fluorescence microscopy to study intracellular signaling in bacteria. *Annual Review of Microbiology*, *64*(1), 373–390. https://doi.org/10.1146/annurev.micro.112408.134205

Khorasani, M. Y., Langari, H., Sany, S. B. T., Rezayi, M., & Sahebkar, A. (2019). The role of curcumin and its derivatives in sensory applications. *Materials Science and Engineering: C*, *103*, 109792. https://doi.org/10.1016/j.msec.2019.109792

Li, K., Ren, T.-B., Huan, S., Yuan, L., & Zhang, X.-B. (2021). Progress and perspective of solid-state organic fluorophores for biomedical applications. *Journal of the American Chemical Society*, *143*(50), 21143–21160. https://doi.org/10.1021/jacs.1c10925

Lv, H.-S., Huang, S.-Y., Zhao, B.-X., & Miao, J.-Y. (2013). A new rhodamine B-based lysosomal pH fluorescent indicator. *Analytica Chimica Acta*, *788*, 177–182. https://doi.org/10.1016/j.aca.2013.06.038

Miletto, I., Gilardino, A., Zamburlin, P., Dalmazzo, S., Lovisolo, D., Caputo, G., Viscardi, G., & Martra, G. (2010). Highly bright and photostable cyanine dye-doped silica nanoparticles for optical imaging: Photophysical characterization and cell tests. *Dyes and Pigments*, *84*(1), 121–127. https://doi.org/10.1016/j.dyepig.2009.07.004

Mukherjee, N., Gaur, R., Shahabuddin, S., & Chandra, P. (2022). Recent progress in lysosome-targetable fluorescent BODIPY probes for bioimaging applications. *Materials Today: Proceedings*, *62*, 7082–7087. https://doi.org/10.1016/j.matpr.2022.01.220

Pendergrass, W., Wolf, N., & Poot, M. (2004). Efficacy of MitoTracker Green and CMXrosamine to measure changes in mitochondrial membrane potentials in living cells and tissues. *Cytometry*, *61A*(2), 162–169. https://doi.org/10.1002/cyto.a.20033

Qi, J., Duan, X., Cai, Y., Jia, S., Chen, C., Zhao, Z., Li, Y., Peng, H.-Q., Kwok, R. T. K., Lam, J. W. Y., Ding, D., & Tang, B. Z. (2020). Simultaneously boosting the conjugation, brightness and solubility of organic fluorophores by using AIEgens. *Chemical Science*, *11*(32), 8438–8447. https://doi.org/10.1039/D0SC03423A

Ragazzi, M., Piana, S., Longo, C., Castagnetti, F., Foroni, M., Ferrari, G., Gardini, G., & Pellacani, G. (2014). Fluorescence confocal microscopy for pathologists. *Modern Pathology*, *27*(3), 460–471. https://doi.org/10.1038/modpathol.2013.158

Ren, J., Zhang, P., Liu, H., Zhang, C., Gao, Y., Cui, J., & Chen, J. (2020). Single-dye-doped fluorescent nanoprobe enables self-referenced ratiometric imaging of hypochlorous acid in lysosomes. *Sensors and Actuators B: Chemical*, *304*, 127299. https://doi.org/10.1016/j.snb.2019.127299

Schultz, M., Müller, R., Ermakova, Y., Hoffmann, J., & Schultz, C. (2022). Membrane-permeant, bioactivatable coumarin derivatives for in-cell labelling. *ChemBioChem*, *23*(6). https://doi.org/10.1002/cbic.202100699

Shen, Q., Wang, S., Yang, N.-D., Zhang, C., Wu, Q., & Yu, C. (2020). Recent development of small-molecule organic fluorophores for multifunctional bioimaging in the second near-infrared window. *Journal of Luminescence*, *225*, 117338. https://doi.org/10.1016/j.jlumin.2020.117338

Shi, C.-E., You, C.-Q., & Pan, L. (2019). Facile formulation of near-infrared light-triggered hollow mesoporous silica nanoparticles based on mitochondria targeting for on-demand chemo/photothermal/photodynamic therapy. *Nanotechnology*, *30*(32), 325102. https://doi.org/10.1088/1361-6528/ab1367

Shi, X.-L., Mao, G.-J., Zhang, X.-B., Liu, H.-W., Gong, Y.-J., Wu, Y.-X., Zhou, L.-Y., Zhang, J., & Tan, W. (2014). Rhodamine-based fluorescent probe for direct bio-imaging of lysosomal pH changes. *Talanta*, *130*, 356–362. https://doi.org/10.1016/j.talanta.2014.07.030

Sung, Y. K., & Kim, S. W. (2020). Recent advances in polymeric drug delivery systems. *Biomaterials Research*, *24*(1), 12. https://doi.org/10.1186/s40824-020-00190-7

Terai, T., & Nagano, T. (2008). Fluorescent probes for bioimaging applications. *Current Opinion in Chemical Biology*, *12*(5), 515–521. https://doi.org/10.1016/j.cbpa.2008.08.007

Van der Velden, J. L., Bertoncello, I., & McQualter, J. L. (2013). LysoTracker is a marker of differentiated alveolar type II cells. *Respiratory Research*, *14*(1), 123. https://doi.org/10.1186/1465-9921-14-123

Xia, Q., Feng, S., Hong, J., & Feng, G. (2021). One probe for multiple targets: A NIR fluorescent rhodamine-based probe for ONOO− and lysosomal pH detection in live cells. *Sensors and Actuators B: Chemical*, *337*, 129732. https://doi.org/10.1016/j.snb.2021.129732

Yang, Z., Sharma, A., Qi, J., Peng, X., Lee, D. Y., Hu, R., Lin, D., Qu, J., & Kim, J. S. (2016). Super-resolution fluorescent materials: an insight into design and bioimaging applications. *Chemical Society Reviews*, *45*(17), 4651–4667. https://doi.org/10.1039/C5CS00875A

Zhang, T., Ma, C., Sun, T., & Xie, Z. (2019). Unadulterated BODIPY nanoparticles for biomedical applications. *Coordination Chemistry Reviews*, *390*, 76–85. https://doi.org/10.1016/j.ccr.2019.04.001

Zhang, X.-F., Wang, T.-R., Cao, X.-Q., & Shen, S.-L. (2020). A near-infrared rhodamine-based lysosomal pH probe and its application in lysosomal pH rise during heat shock. *Spectrochimica Acta Part A: Molecular and Biomolecular Spectroscopy*, *227*, 117761. https://doi.org/10.1016/j.saa.2019.117761